
LIFT AND DRAG ON BLUFF BODIES IN A WIND TUNNEL

YANNICK BONDO

Student ID: 50235476

University at Buffalo

MAE 339

In Collaboration with: N/A

9/29/2021

CONTENTS

Abstract	2
Introduction	3
Methods	7
Result and discussion	12
Conclusion.....	19
Reference.....	20
Appendix.....	21

ABSTRACT

A wind tunnel is an important tools that aids engineers in determining aerodynamic performances of a body, such as an airfoil. Notably, the aerodynamic performance of a body is closely dependent on the characteristic of the free-stream velocity flowing over said body. Therefore, to be able to capture those performances, that is by way of measurement, engineers utilizes various measuring devices, in our case being the force balance, to capture the relationship between the lift and drag force with respect to the angle of attack. Theoretically, the force is directly proportional to pressure, with this in mind, we were able to study the pressure distribution across the airfoils, namely the NACA 0012 and NACA 4412, thereby determining the lift and drag coefficient acting on it. Markedly, nondimensionalizing the arbitrary points along the chord length helped us better understand the relationship between the moment coefficient with respect to the angle of attack. Lastly, the efficiency and accuracy of our results can be improved by collecting a larger sample of data and by using digital manometer for measuring the heights on the manometer for eradicating bias error.

INTRODUCTION

In this lab we performed experiments in a wind tunnel to investigate the aerodynamics characteristics of lift and drag, on bluff and streamlined bodies. Unfortunately, the drag-axis on our force transducer seem to have misbehaved on experiment day, thus we are limiting our analysis to the aerodynamic characteristic of lift, omitting all drag data we may have gathered.

Notably, we performed three experiments in our wind tunnel. Our first experiment consisted measuring the free-stream velocity inside the wind tunnel test section using a pitot-static probe at different fan frequencies. Our Second experiment required that we measure the lift and drag force using a force balance on a NACA 0012 airfoil at different angles of attack. And our last experiment required that we measure the pressure distribution of the NACA 4412 at different angle of attack (AOA) to find the lift coefficient, the leading edge moment coefficient, and the location of the center of pressure for the NACA 4412 airfoil.

Theory

As fluids flow around a body, exerting a force on it, lift is the component of the force perpendicular to the oncoming flow, and in aerodynamics it is that force that supports a body against the action of gravity. An airfoil for that matter, extract lift from the pressure difference across the lower and the upper surface of the airfoil, with the lift being positive when the pressure acting on the lower surface is greater than the pressure acting on the upper surface, and conversely so. Generally, the resultant force (per unit span) acting on the airfoil, F , is equal to the negative of the closed integral of the pressure, P , around the airfoil surface, S :

$$F = - \oint P \mathbf{n} dS \quad (1)$$

Where n is the unit vector of the surface S . Thus, for a thin airfoil (that is an airfoil where the thickness above the mean camber line is much less smaller than the chord length) much like our NACA 0012 would have the force, F , acting on it approximated by:

$$F = - \left(\int_c^0 P_u(-dx) + \int_0^c P_l(-dx) \right) = \int_0^c (P_l - P_u) dx \quad (2)$$

Where c is the chord length, x is the distance from the leading edge, and P_l and P_u are the pressure acting the lower and upper surface, respectively. The lift, L , is the vertical component of the force, F :

$$L = F \cos \alpha \quad (3)$$

This is shown schematically in figure 1, where α is the angle of attack and V_∞ is the free-stream velocity, and the Drag force, D , is the projection of the force, F , onto the horizontal direction: $D = F \sin \alpha$

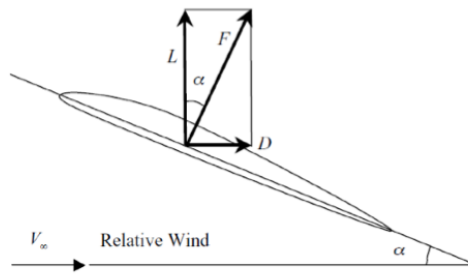


Figure 1: The airfoil force schematic

The moment about the leading edge, M_{LE} , is generally defined by the following approximated equation:

$$M_{LE} = \int_0^c x(P_l - P_u) dx \quad (4)$$

By defining equation 2-4 in terms of dimensionless coefficient we going to get these expressions below:

$$C_F = \frac{F}{q_\infty c} \quad C_L = \frac{L}{q_\infty c} = C_F \cos \alpha \quad C_{M,LE} = \frac{M_{LE}}{q_\infty c^2} \quad (5)$$

The relations on the previous page are per unit span and the quantity q_∞ is the free-stream dynamic pressure:

$$q_\infty = \frac{1}{2} \rho_\infty V_\infty^2 \quad (6)$$

Where ρ_∞ is the free-stream density. We further define the upper and lower surface coefficients, $C_{p,l}$ and $C_{p,u}$, respectively as:

$$\frac{P_l - P_u}{q_\infty} = \frac{P_l - P_\infty}{q_\infty} - \frac{P_u - P_\infty}{q_\infty} \equiv C_{p,l} - C_{p,u} \quad (7)$$

Where P_∞ is the reference pressure. Then Equation (2) and (4) takes the following non-dimensional forms:

$$C_F = \int_0^c \frac{P_l - P_u}{q_\infty c} d\left(\frac{x}{c}\right) = \int_0^1 (C_{p,l} - C_{p,u}) d\xi \quad (8)$$

$$C_{M,LE} = - \int_0^c \left(\frac{x}{c}\right) \frac{P_l - P_u}{q_\infty c} d\left(\frac{x}{c}\right) = - \int_0^1 \xi (C_{p,l} - C_{p,u}) d\xi \quad (9)$$

Where $\xi = \left(\frac{x}{c}\right)$ is the fractional dimensionless distance along the chord length.

The resultant force acts at some point along the chord length called the center of pressure. This distance predicts that if ξ_{CP} is multiplied by C_F , then the resultant

would be a moment equal to Equation (9). Thus, if C_F and $C_{M,LE}$ are known independently, like from experimental data, then ξ_{CP} may be found with the following relationship:

$$C_{M,LE} = -\xi_{CP}C_F \longrightarrow \xi_{CP} = -\frac{C_{M,LE}}{C_F} \quad (10)$$

Knowing ξ_{CP} makes it possible for the moment coefficient, C_M , about any other point ξ along the chord to be calculated as:

$$C_M = -(\xi_{CP} - \xi) C_F \quad (11)$$

Markedly, there is a point along the chord length about which the moment coefficient is constant with angle of attack (AOA); this is called the aerodynamic center and may be calculated from the previous equation as:

$$\xi_{AC} = \xi_{CP} + \frac{C_{M,AC}}{C_F} \quad (12)$$

Where $C_{M,AC}$ is the moment coefficient about the aerodynamic center. Ordinarily, the location of the center of pressure and aerodynamic center do not coincide along the same point. Although, for low speed, thin airfoil, much like the NACA 0012, these two points are so close to each other that it is often assumed that they coexist on the same point.

METHODS

Equipment: Wind Tunnel (Experiment 1.)

The experiments is conducted in a low-speed, Eiffel- type tunnel constructed by Engineering Laboratory Design, Inc. (ELD), with the test section cross-section of 12"×12"(30.48 cm × 30.48 cm) and a length of 24"(60.96 cm) (see Figure 2 schematic). Air is drawn into the inlet through a honeycomb and screen pack, for flow-straightening and to suppress velocity fluctuations, and is accelerated through into the test section.

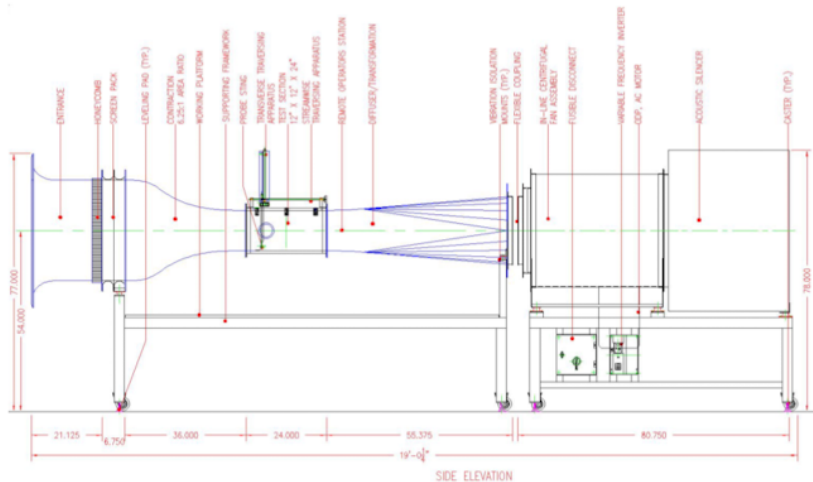


Figure 2: Schematic of the wind tunnel, taken from the ELD,Inc., literature.

Procedures

1. We moved the pitot-static probe in the middle of test-section of the tunnel facing forward.
2. We started the tunnel 15Hz and waited for a couple seconds to have the flow stabilize.
3. We measured the differential pressure correlating with our fan frequency using LabVIEW VI and calculated the free-stream velocity by massaging Equation (6) a bit.
4. We repeated the same procedure for increments of 5Hz till we reached a frequency of 40Hz.

Equipment: Force Balance (Experiment 2)

In a wind tunnel, a force balance is among one of the possible instruments used for determining the force on a body, namely lift force, L , and drag force, D . As shown by figure 3, a force balance consist of a black fairing that extends up into the test section and this piece is basically a streamlined cap shielding a sting (a silver-colored shaft) from the aerodynamic force of the tunnel free-stream. The airfoil model is screwed on the sting at a desired angle of attack and as the oncoming flow comes in contact with our model, there will be a very slight deviation in the sting position which is sent to a specialize thin-beam structure within the force balance housing. This deflection is then converted into a voltage that can be measured by via an LVDT sensor attached between the beam assemblies and the force balance housing. An LVDT is an electromechanical device that converts mechanical motion into a variable voltage signal, and vice versa. The outputted voltage signal is sent to the data acquisition box (DAQ) where it is amplified and conditioned. The amplified signal is then converted into a digital signal and recorded on LabVIEW.

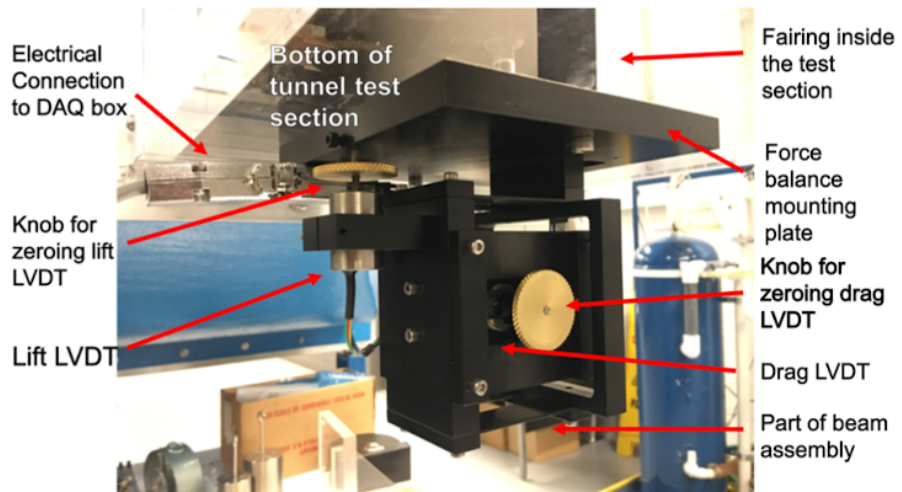


Figure 3: Force balance mounted on a wind tunnel.

Equipment: Measuring the angle of attack (AOA) in the lab fixed frame using a Camera. (Experiment 2)

This experiment is conducted by capturing the instantaneous angular position of the NACA 0012 with a Camera, then loading the image on GIMP and measuring the angle of attack (see figure 4 on the next page).

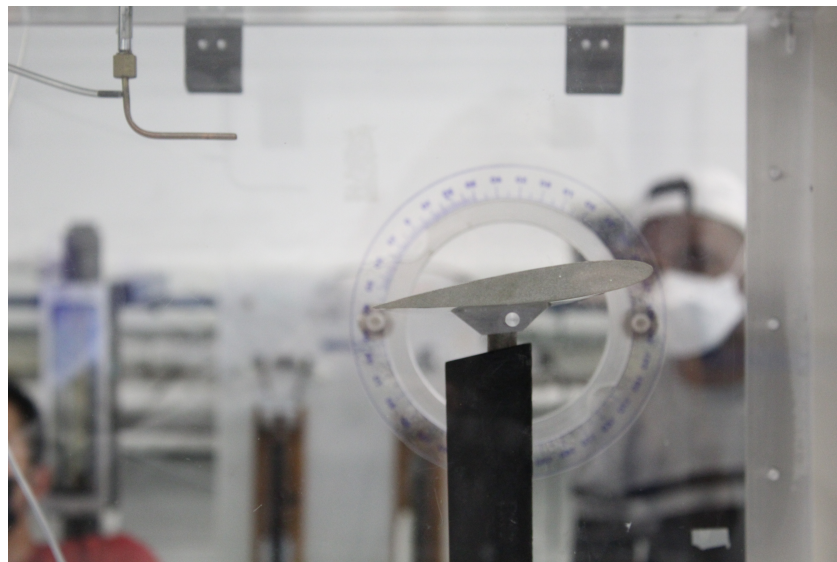


Figure 4: A photo of the instantaneous angle of attack of the NACA 0012

Procedure

1. We installed the NACA 0012 airfoil using a long handled Allen wrench and mounted our model onto the sting. Then we very carefully screwed it in
2. We setting our airfoil to some angle of attack as shown on figure 4. We captured that position and measured that angle of attack via GIMP, then recorded it.
3. We ran our wind tunnel to 25 Hz and measured the Lift and drag force with the “Wind Tunnel DAQ_2019” VI.
4. Then we repeated step 2 and 3 at six different angles, making that one of our angles is past the stall angle.

Equipment: Manometer Bank (Experiment 3.)

The manometer bank are series of columns housing a manometer fluid (specific gravity=0.826) with the top of the manometer connected to tubing (see figure 5), which is later connected to the airfoil in correspondence with the alignment of pressure taps situated along the top and bottom of the airfoil (see figure 6). As the free-stream flow along the airfoil at some angle of attack, the pressure along the airfoil change, and a reduction in static pressure anywhere on the airfoil will lead the height of the gage fluid to increase, as they're connected to a pressure tap. Reading and recording the height of each column would help us develop a pressure profile of the airfoil. (For a manometer $P = \rho hg$)

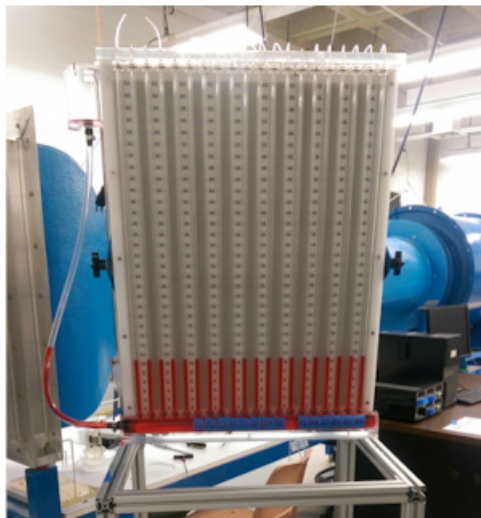


Figure 5: Manometer Bank

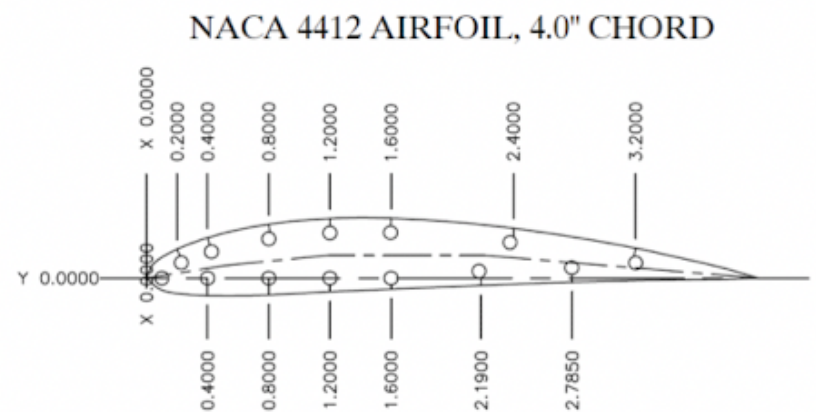


Figure 6: Pressure tap location in inches from the leading edge of NACA 4412 airfoil

Procedure

1. We mounted the NACA 4412 2-D airfoil to a plexiglass wall plug and fitted with a small brass pin at the opposite end. The airfoil consists of an array of eight (8) pressure taps located on the upper surface and six (6) pressure taps are located on the bottom surface as shown by figure 6.

2. We connected the tubes in accordance with their array alignment, that is the connecting the 8 tubes on the manometer bank to the top surface of the airfoil, and the 6 tubes to the bottom of the surface of the airfoil (see figure 7).
3. We then set the airfoil at some angle of attack and measured the angle with a camera and recorded it.
4. We measured the height of the atmospheric reading. Then ran our wind tunnel at 25 Hz and measured the other 14 heights of the gage fluid.
5. We turned off our wind tunnel and repeated step 3 and 4 for six different angles of attack within the range of -10° to 15° .

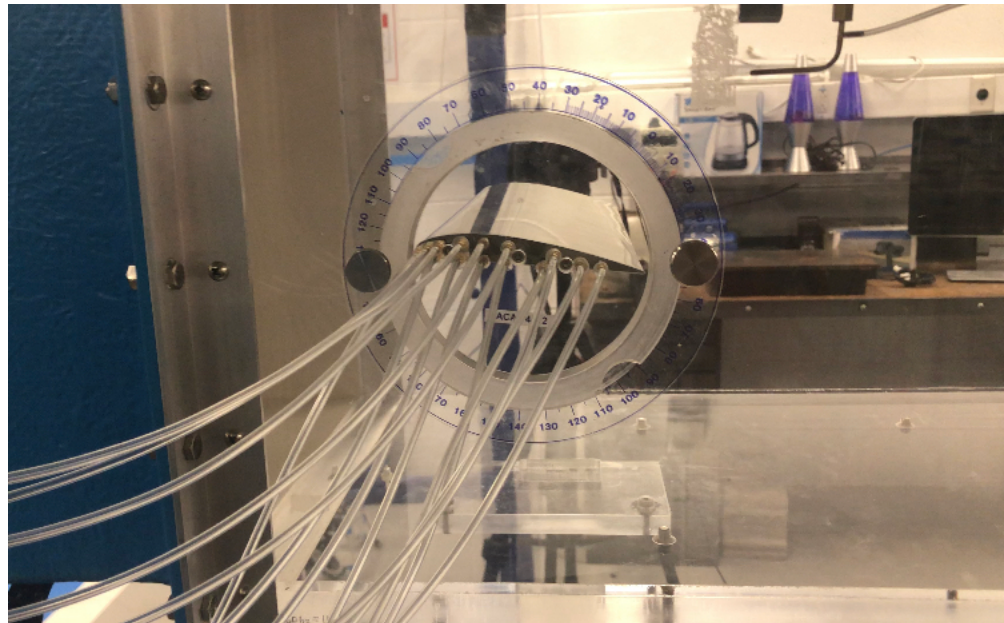


Figure 7: A photo of the pressure tube connection on the NACA 4412 airfoil

RESULTS AND DISCUSSION

Part 1: Measuring the free-stream velocity.

Results.

For part 1, we used a pitot-static tube to measure the dynamic pressure at different frequencies, then used Equation (6) to find the free-stream velocity.

Table 1: The wind tunnel free-stream velocity at respective fan frequencies

Frequency (Hz)	0	15	20	25	30	35	40
V_∞ (m/s)	0	6.263	12.692	18.16	23.435	28.557	33.641

Discussion.

By looking at our results on Table 1, we can observe that the speed of the free-stream velocity increased with increasing frequency.

Part 2: Measuring the lift and drag force of the NACA 0012 using a force balance at different angle of attack.

Results.

For part 2, we measured the lift force acting on the NACA 0012 airfoil at 6 different angles of attack at a frequency of 25 Hz with one angle above the stall point of $+12^\circ$, then computed for the lift (per unit span), L' , and the coefficient of lift, C_L (see Appendix for show of work).

Table 2: The Lift (per unit span), L' , and coefficient of lift, C_L , at respective angles of attack

Angle of attack (degrees)	1.85	3.89	4.82	7.75	9.92	13.21
L' (N/m)	8.3727	13.4514	15.3576	20.4364	24.2454	15.3576
C_L	0.0056	0.0089	0.0102	0.0136	0.0161	0.0102

To test the validity of our results, we calculated the Reynolds number (Re) at free-stream velocity corresponding with the frequency of 25 Hz, then extracted

relevant data from www.airfoiltools.com at our calculated Reynolds number then plotted our experimental data with the airfoil data. (see Appendix for show of work.)

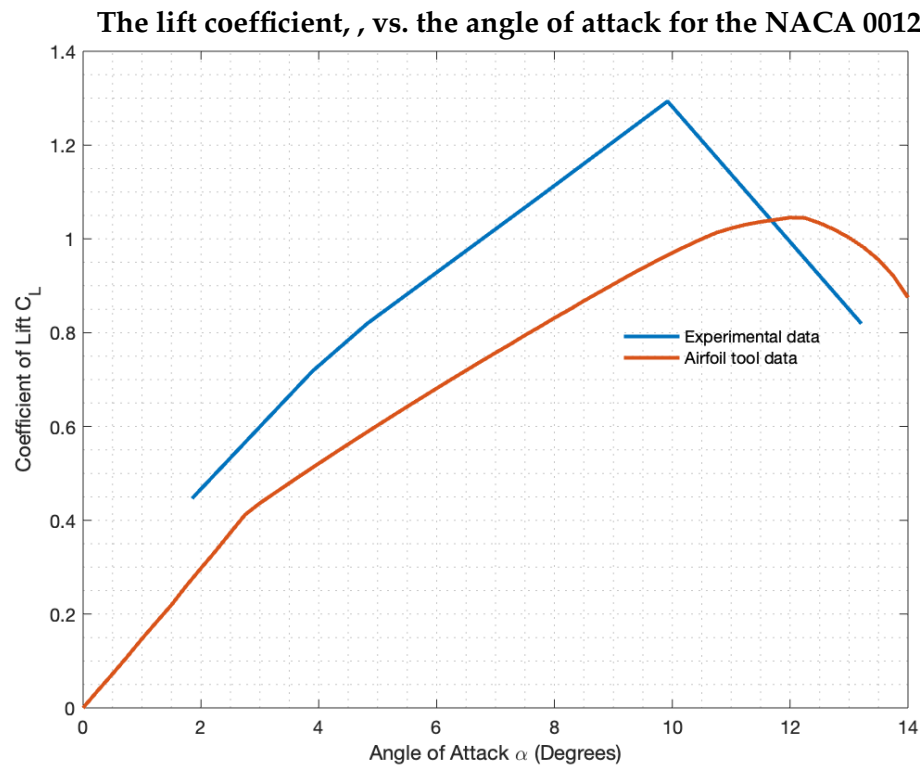


Figure 7: The lift coefficient, C_L vs. the angle of attack (AOA) for the NACA 0012 airfoil.

Discussion

From figure 7, we can notice that our experimental data and the airfoil tool data are not superimposed, that is they are not following each other closely, due to the nature of the experiment; as we collected data for only six angles compared to the thousands of angles sampled in the airfoil tool data. However, we can observe the same trend for both data set. We can evidently see that the lift coefficient, C_L , increases with increasing angle of attack (meaning that a high amount of lift is being produced with increasing angle of attack) until reaching the stall angle of 12° ; then we have our lift coefficient, C_L , decreasing for any angle of attack above 12° . This decrease happens as a result of the airfoil crossing

the critical angle threshold (called the stall point), increasing the flow separation between the higher and lower surface of the airfoil and resulting to a loss of lift.

Part 3: Measuring the surface pressure distribution on the NACA 4412 with a Manometer bank.

Results

For part 3, we measured the surface pressure distribution on the NACA 4412 airfoil via manometer bank at 6 different angles of attack, while running the wind tunnel at a frequency of 25 Hz. Then computed for the non-dimensional coefficient pressure, C_P , across the non-dimensional tap location ξ (see Appendix for show of work).

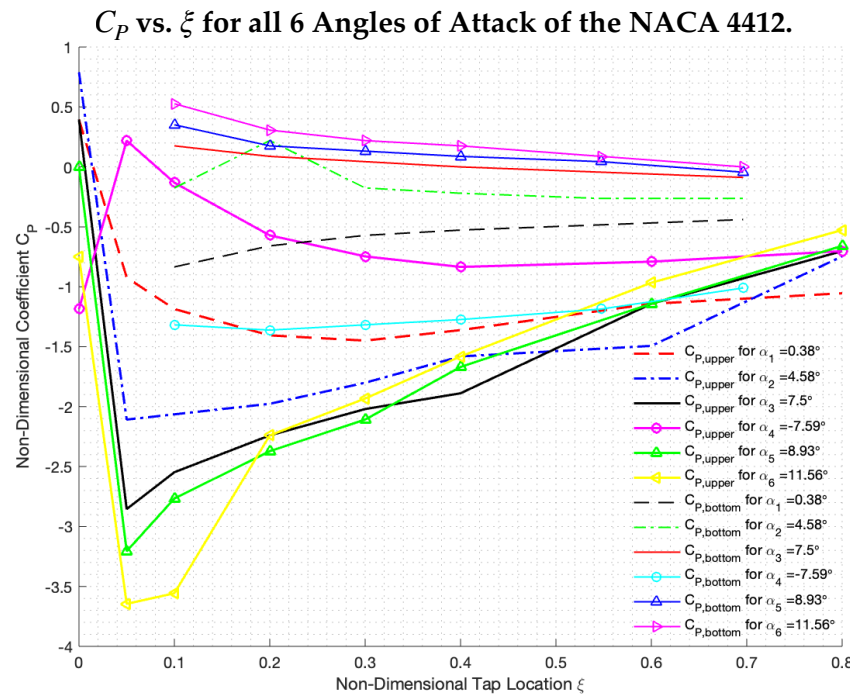


Figure 8: The NACA4412 Pressure coefficient vs. non-dimensional Tap location for each angle of attack.

Discussion

From figure 8, We observe that for every positive angle of attack on the upper surface of our airfoil, we have the trend-line initially tending negative then

gradually increases converging toward zero the farther we move from the leading edge. And we further observe that for positive angles on the lower surface of the airfoil, we have the trend-line initially tending positive then decreases converging toward zero the farther we move from the leading edge. Notably, we have the opposite occurrence for negative angles of attack. This phenomenon happens because the pressure at the trailing edge of the airfoil aims to equal that of the free-stream, leading the pressure coefficient to head toward zero.

Results

Using Matlab, we integrated the coefficient of pressure consistent with Equation (8) using trapezoidal rule of integration to solve for C_F , then used Equation (5) to compute for the lift Coefficient. We plotted our experimental results juxtaposed to the Airfoil tool data and theoretical lift trend (see appendix for derivation and show of work).

NACA 4412 Coefficient of Lift, C_L , vs. Angle of Attack, α

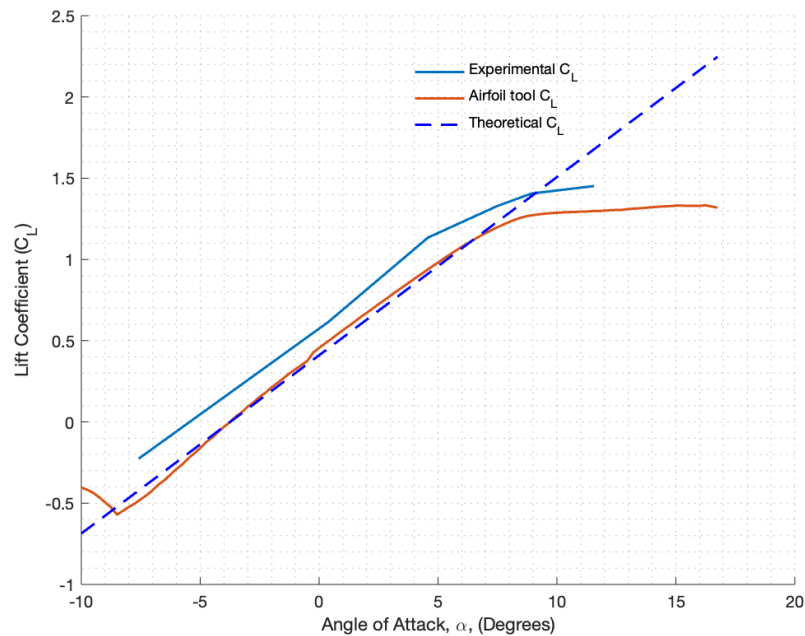


Figure 9: The NACA4412 Lift coefficient vs. Angle of attack.

Discussion

From figure 9, we can see that our experimental data and the airfoil tool data are not superimposed, but are relatively close, maybe due to the nature of the experiment; as we collected data for only six angles compared to the thousands of angles sampled in the airfoil tool data. Markedly, has we compared our lift coefficient to the theoretical lift trend, we observe that our trend-line seem to have a slope of 2π . That being consistent we Anderson's theory as stipulated that, in order to have a symmetric airfoil, the slope of theoretical lift should equal $2\pi \text{ rad}^{-1}$, leading the lift coefficient to be linearly promotional to the angle of attack. In addition, the lift coefficient both the experimental data and the airfoil tool data is seem to trend constant (we are assuming that it will eventually go down) for every angle above the stall point.

Results

Using Matlab, we integrated the coefficient of pressure consistent with Equation (9) using trapezoidal rule of integration to solve for the coefficient of moment about the leading edge $C_{M,LE}$ (see appendix for show of work).

NACA 4412 Coefficient of Moment about the Leading Edge, $C_{M,LE}$, vs. Angle of Attack, α

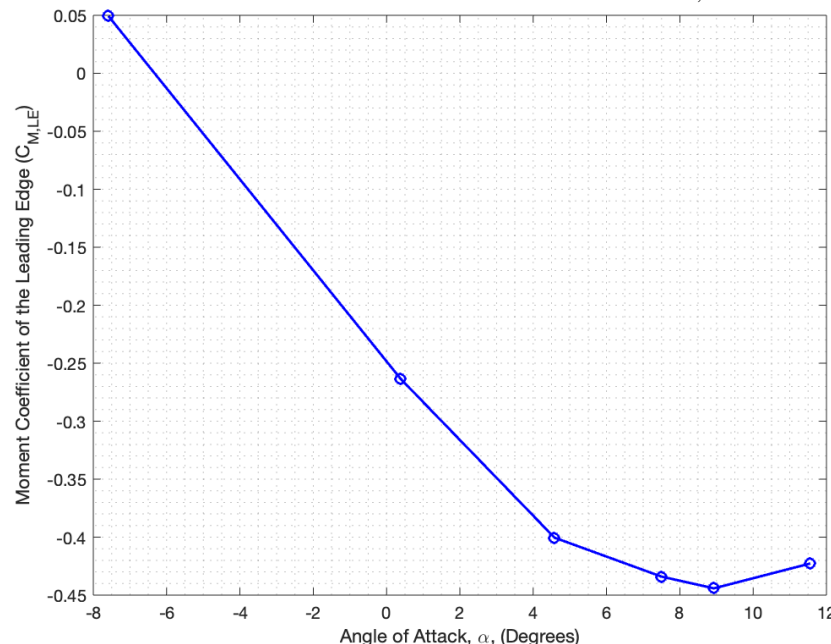


Figure 10: The NACA4412 Moment coefficient about the leading edge vs. Angle of attack.

Discussion

From figure 10, we can observe that the moment coefficient about the leading edge decreases with increasing angle of attack until hitting the stall angle, then we have our trend-line reverse course, increasing with every the angle of attack above the stall point. This trend happens because as the angle of attack increase, the lift on the leading edge of the airfoil grows more slowly relative to lift on the trailing edge of the wing since there coefficient of lift is larger on the leading edge is larger than that on the trailing edge.

Results

Using Equation (12) we calculated for coefficient of moment about the aerodynamic center and plotted our results below (see appendix to for show of work).

NACA 4412 Coefficient of Moment about the Aerodynamic Center $C_{M,AC}$ vs. Angle of Attack α

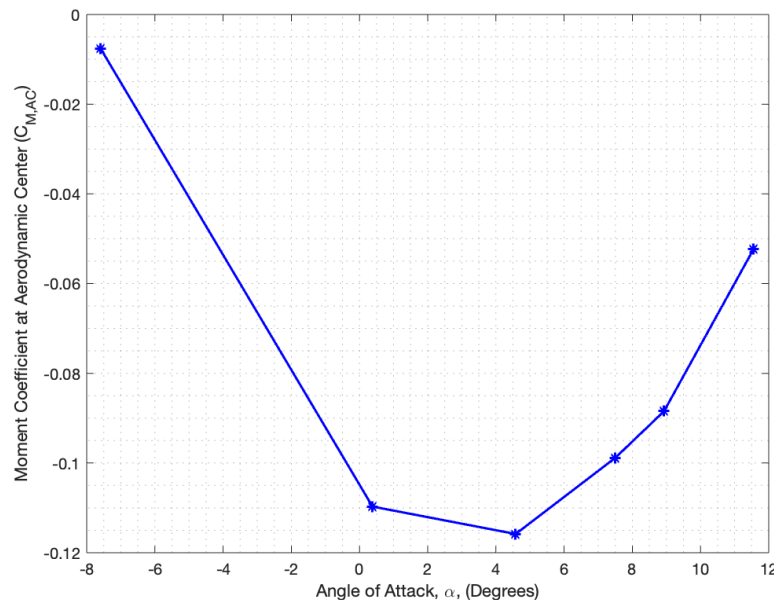


Figure 11: The NACA4412 Moment coefficient about the Aerodynamic center vs. Angle of attack.

Discussion

From figure 11, we observe that the moment coefficient about the aerodynamic pressure is in fact changing with angle of attack, that is our moment coefficient is

decreasing with every increase in angle of attack till reaching the stall angle, then it reverses direction. Therefore, with respect to the thin airfoil theory, this shows for the NACA 4412 airfoil, the location of the aerodynamic center and the center pressure do not coincide. Since the slope of the coefficient of moment for the aerodynamic center doesn't equal to zero.

CONCLUSION

In our experiment, we utilized various approaches to solving some aerodynamics characteristics, namely the coefficient of lift (and drag), and the coefficient moments cross our symmetrical airfoils. We performed three experiments in a wind tunnel, we the first experiment consisting of measuring the free-stream velocity inside the wind tunnel test section using a pitot-static probe at different fan frequencies, the Second experiment demanding that we measure the lift and drag force using a force balance on a NACA 0012 airfoil at different angles of attack, and the last experiment demanding that we measure the pressure distribution of the NACA 4412 at different angle of attack (AOA) to find the lift coefficient, the leading edge moment coefficient, and the location of the center of pressure for the NACA 4412 airfoil. And concluded that, our results seemed to be consistent with the predictions from theory. In addition, we compared our experimental results to well established data from www.Airfoiltools.com to test the validity of our result. By and large, this experiment provided us we a better understanding of the underlining theory of aerodynamic, as well as, attest to the accuracy and reliability of different experimental technique that the field of experimental aerodynamic has to offer.

REFERENCE

- [1] Burge, M. (2020) Lift and Drag on bluff bodies in a wind tunnel. Buffalo, NY: University at Buffalo.
- [2] Anderson, J. D. (2011). Fundamentals of aerodynamics (6th ed.). New York, NY: McGrawHill.

APPENDIX

Relevant Matlab Code

```

clear; close all
%% PART 2 NACA0012 USING A FORCE BALANCE
U_inf=18.15970261;
nu=1.5e-5;
c=10.16e-2;
b=30.48e-2;
S=b*c;
rho_inf=1.119;
dp=.5*rho_inf*U_inf^2;
L=[2.552 4.1 4.681 6.229 7.39 4.681];

AOA=[1.85 3.89 4.82 7.75 9.92 13.21];
AOA_new=[0 0.25 0.5 0.75 1 1.25 1.5 1.75 2 2.25 2.5 2.75
3 3.25...
3.5 3.75 4 4.25 4.5 4.75 5 5.25 5.5 5.75 6 6.25
6.5 6.75...
7 7.25 7.5 7.75 8 8.25 8.5 8.75 9 9.25 9.5 9.75
10 10.25...
10.5 10.75 11 11.25 11.5 11.75 12 12.25 12.5...
12.75 13 13.25 13.5 13.75 14];
c_Lnew=[0 0.037 0.0724 0.1093 0.1475 0.1837 0.2196...
0.2601 0.2976 0.3346 0.3736 0.412 0.4365 0.4579 0.4792 0.5003
0.5212...
0.5418 0.5623 0.5825 0.6026 0.6225 0.6422 0.6617 0.6812 0.7005
0.7195...
0.7385 0.7571 0.7753 0.7946 0.8125 0.8315 0.8489 0.8678 0.8855
0.9031...
0.921 0.9379 0.9542 0.9703 0.9853 0.9999 1.0133 1.0227 1.0305
1.0363...
1.0408 1.0454 1.0447 1.0338 1.0198 1.0026 0.9817 0.9556 0.9215
0.8751];

Rec=(U_inf*c)/(nu);
L_span=L/b;
c_L=(L_span)/(dp*c);

plot(AOA,c_L,AOA_new,c_Lnew,'linewi',2)
xlabel('Angle of Attack \alpha (Degrees)');ylabel('Coefficient of Lift C_L');
% title('NACA 0012 Lift Coefficient vs. Angle of Attack')
legend('Experimental data','Airfoil tool data')
legend('boxoff')
grid minor

%% PART 3 NACA4412 USING A MANOMETER BANK
c_m= 10.16e-2;
Re_in=(U_inf*c_m)/(nu);
c_b=4;

```

```

U_tap=[0 .2 .4 .8 1.2 1.6 2.4 3.2];
L_tap=[0 .4 .8 1.2 1.6 2.19 2.785];
xi_u=U_tap/c_b;
xi_l=L_tap/c_b;
xi_l(1)=[];
gamma=0.826*1000*9.81;

h_ua1=[ 7.9   10.9    11.5    12   12.1    11.9    11.4    11.2].*10^-2;
h_ua2=[ 7     13.6    13.5    13.3   12.9    12.4    12.2    10.5].*10^-2;
h_ua3=[ 7.9   15.3    14.6    13.9   13.4    13.1    11.4    10.4].*10^-2;
h_ua4=[11.5   8.3   9.1   10.1    10.5   10.7    10.6    10.4].*10^-2;
h_ua5=[ 8.8   16.1    15.1    14.2   13.6    12.6    11.4    10.3].*10^-2;
h_ua6=[10.5   17.1    16.9    13.9   13.2    12.4    11   10].*10^-2;

h_ba1=[10.7   10.3    10.1    10   9.9   9.8].*10^-2;
h_ba2=[ 9.2   8.3   9.2   9.3   9.4   9.4].*10^-2;
h_ba3=[ 8.4   8.6   8.7   8.8   8.9   9].*10^-2;
h_ba4=[11.8   11.9    11.8    11.7   11.5    11.1].*10^-2;
h_ba5=[ 8     8.4   8.5   8.6   8.7   8.9].*10^-2;
h_ba6=[ 7.6   8.1   8.3   8.4   8.6   8.8].*10^-2;
h_infal=-8.8*10^-2;

c_pual=(( -h_ua1-h_infal).*gamma)./(dp);
c_pua2=(( -h_ua2-h_infal).*gamma)./(dp);
c_pua3=(( -h_ua3-h_infal).*gamma)./(dp);
c_pua4=(( -h_ua4-h_infal).*gamma)./(dp);
c_pua5=(( -h_ua5-h_infal).*gamma)./(dp);
c_pua6=(( -h_ua6-h_infal).*gamma)./(dp);

c_pba1=(( -h_ba1-h_infal).*gamma)./(dp);
c_pba2=(( -h_ba2-h_infal).*gamma)./(dp);
c_pba3=(( -h_ba3-h_infal).*gamma)./(dp);
c_pba4=(( -h_ba4-h_infal).*gamma)./(dp);
c_pba5=(( -h_ba5-h_infal).*gamma)./(dp);
c_pba6=(( -h_ba6-h_infal).*gamma)./(dp);

hold on
plot(xi_u,c_pual,'r--','linewi',1.5)
plot(xi_u,c_pua2,'b-.','linewi',1.5)
plot(xi_u,c_pua3,'k-','linewi',1.5)
plot(xi_u,c_pua4,'m-o','linewi',1.5)
plot(xi_u,c_pua5,'g-^','linewi',1.5)
plot(xi_u,c_pua6,'y-<','linewi',1.5)

plot(xi_l,c_pba1,'k--','linewi',1)
plot(xi_l,c_pba2,'g-.','linewi',1)
plot(xi_l,c_pba3,'r-','linewi',1)
plot(xi_l,c_pba4,'c-o','linewi',1)
plot(xi_l,c_pba5,'b-^','linewi',1)
plot(xi_l,c_pba6,'m->','linewi',1)

% title('C_{P} vs. \xi for the Largest and smallest Angle of Attack of the
NACA 4412.')

```

```

xlabel('Non-Dimensional Tap Location \xi'); ylabel('Non-Dimensional
Coefficient C_{P}')
```

```

legend('C_{P,upper} for \alpha_1 =0.38\circ', 'C_{P,upper} for \alpha_2
=4.58\circ', 'C_{P,upper} for \alpha_3 =7.5\circ', 'C_{P,upper} for \alpha_4
=-7.59\circ', 'C_{P,upper} for \alpha_5 =8.93\circ', 'C_{P,upper} for \alpha_6
=11.56\circ', 'C_{P,bottom} for \alpha_1 =0.38\circ', 'C_{P,bottom} for
\alpha_2 =4.58\circ', 'C_{P,bottom} for \alpha_3 =7.5\circ', 'C_{P,bottom} for
\alpha_4 =-7.59\circ', 'C_{P,bottom} for \alpha_5 =8.93\circ', 'C_{P,bottom}
for \alpha_6 =11.56\circ')
grid minor
legend('boxoff')
hold off

CFA1=trapz(xi_l,c_pba1)-trapz(xi_u,c_pua1);
CFA2=trapz(xi_l,c_pba2)-trapz(xi_u,c_pua2);
CFA3=trapz(xi_l,c_pba3)-trapz(xi_u,c_pua3);
CFA4=trapz(xi_l,c_pba4)-trapz(xi_u,c_pua4);
CFA5=trapz(xi_l,c_pba5)-trapz(xi_u,c_pua5);
CFA6=trapz(xi_l,c_pba6)-trapz(xi_u,c_pua6);
CF=[CFA4 CFA1 CFA2 CFA3 CFA5 CFA6];

AOA_part3=[-7.59 .38 4.58 7.5 8.93 11.56];
CLA1=CFA1*cosd(0.38);
CLA2=CFA2*cosd(4.58);
CLA3=CFA3*cosd(7.5);
CLA4=CFA4*cosd(-7.59);
CLA5=CFA5*cosd(8.93);
CLA6=CFA6*cosd(11.56);

AOA_npart3=[-10 -9.75 -9.5 -9.25 -8.75 -8.5 -8.25 -8 -7.75 ...
-7.5 -7.25 -7 -6.75 -6.5 -6.25 -6 -5.75 -5.5 -5.25 ...
-5 -4.75 -4.5 -4.25 -4 -3.75 -3.5 -3.25 -3 -2.75 ...
-2.5 ...
-2.25 -2 -1.75 -1.5 -1.25 -1 -0.75 -0.5 -0.25 0 ...
0.25 ...
0.5 0.75 1 1.25 1.5 1.75 2 2.25 2.5 2.75 3 3.25 ...
3.5 3.75 ...
4 4.25 4.5 4.75 5 5.25 5.5 5.75 6 6.25 6.5 6.75 ...
7 7.25 7.5 7.75 8 8.25 8.5 8.75 9 9.25 9.5 9.75 ...
10 10.25 10.5 10.75 11 11.25 11.5 11.75 12 12.25 ...
12.5 ...
12.75 13 13.25 13.5 14 14.25 14.5 14.75 15 15.25 ...
15.5 ...
15.75 16 16.25 16.5 16.75];
CL_npart3=[-0.4048 -0.4169 -0.4366 -0.44631 -0.5253 -0.5707 -0.5467 ...
-0.5231 -0.5018 -0.4754 -0.4503 -0.42 -0.385 -0.3579 -0.3232 ...
-0.2905 ...
-0.2604 -0.2238 -0.193 -0.161 -0.1239 -0.0963 -0.0626 -0.0298 -0.0012 ...
0.0341 ...
0.0601 0.0943 0.1208 0.1543 0.1807 0.2125 0.2399 0.2689 0.2984 ...
0.3243 ...
0.3496 0.3752 0.4266 0.4558 0.4826 0.5094 0.5371 0.5649 0.5909 ...
0.6178 ...]

```

```

0.6455 0.6713 0.6976 0.7248 0.7505 0.7765 0.8035 0.8286 0.8545
0.8807...
0.9054 0.9312 0.9563 0.9809 1.0066 1.0303 1.0545 1.078 1.1002
1.1214...
1.1425 1.1625 1.181 1.1982 1.215 1.2308 1.2453 1.2577 1.2668
1.2728...
1.2779 1.2819 1.2847 1.2873 1.2892 1.2911 1.2917 1.2943 1.2947
1.2979...
1.298 1.3002 1.3033 1.3045 1.3053 1.3099 1.313 1.3149 1.3213
1.324...
1.3262 1.3282 1.3308 1.3307 1.3304 1.3299 1.3299 1.3328 1.3257
1.3187];

```

```

CL_part3=[CLa4 CLa1 CLa2 CLa3 CLa5 CLa6];
CL_o=linspace(-.0012, 0.0943 );
AOA_airfoil=linspace(-3.75,-3);
CL_oi=0;
AOA_airfoili=interp1(CL_o,AOA_airfoil,CL_oi,'linear');
CL_theo=(AOA_npart3-AOA_airfoili)*(2*pi^2/180);

hold on
plot(AOA_part3,CL_part3,'linewi',1.5);
plot(AOA_npart3,CL_npart3,'linewi',1.5);
plot(AOA_npart3,CL_theo,'b--','linewi',1.5)
xlabel('Angle of Attack, \alpha, (Degrees)');ylabel('Lift Coefficient
(C_L)'); %title('NACA 4412 Coefficient of Lift, C_L, vs. Angle of Attack,
\alpha');
legend('Experimental C_L','Airfoil tool C_L','Theoretical C_L')
legend('boxoff')
grid minor
hold off

C_Mleal=(-trapz(xi_l,(xi_l.*c_pba1))+trapz(xi_u,(xi_u.*c_pua1)));
C_Mlea2=(-trapz(xi_l,(xi_l.*c_pba2))+trapz(xi_u,(xi_u.*c_pua2)));
C_Mlea3=(-trapz(xi_l,(xi_l.*c_pba3))+trapz(xi_u,(xi_u.*c_pua3)));
C_Mlea4=(-trapz(xi_l,(xi_l.*c_pba4))+trapz(xi_u,(xi_u.*c_pua4)));
C_Mlea5=(-trapz(xi_l,(xi_l.*c_pba5))+trapz(xi_u,(xi_u.*c_pua5)));
C_Mlea6=(-trapz(xi_l,(xi_l.*c_pba6))+trapz(xi_u,(xi_u.*c_pua6)));
C_Mlea=[C_Mlea4 C_Mleal C_Mlea2 C_Mlea3 C_Mlea5 C_Mlea6];
% grid minor

plot(AOA_part3,C_Mlea,'b-o','linewi',1.5)
grid minor
xlabel('Angle of Attack, \alpha, (Degrees)');
ylabel('Moment Coefficient of the Leading Edge (C_{M,LE})'); %title('NACA
4412 Coefficient of Moment of the Leading Edge, C_{M,LE}, vs. Angle of
Attack, \alpha');

xi_cp=-C_Mlea./CF;
C_Mac=(0.25-xi_cp).*CF;
grid minor
plot(AOA_part3,C_Mac,'b-*','linewi',1.5)

```

```
grid minor
xlabel('Angle of Attack, \alpha, (Degrees)');
ylabel('Moment Coefficient at Aerodynamic Center (C_{M,AC})'); %title('NACA
4412 Coefficient of Moment at Aerodynamic Center, C_{M,AC}, vs. Angle of
Attack, \alpha');
```

Relevant derivations

$$\frac{P_L - P_\infty}{P_\infty} = \rho g \frac{h_\infty - h_L}{P_\infty} = 1000 \times gSG \frac{h_\infty - h_L}{P_\infty}$$

$$C_L = 2\pi (\alpha - \alpha_0) \text{ (theoretical lift coefficient)}$$